Abating HCl and HNO3 is more effective than NH3 for mitigating high aerosol loading over the Indo-Gangetic Plain

Prodip Acharja[1], Sachin D. Ghude[1], Bärbel Sinha[2], Mary C Barth[3], Rachana Kulkarni[4], Vinayak Sinha[5], Rajesh Kumar[6], Kaushar Ali[7], Gaurav Govardhan[1], Ismail Gultepe[8], and Madhavan Nair Rajeevan[9]

[1]Indian Institute of Tropical Meteorology
[2]Indian Institute of Science Education and Research Mohali
[3]National Center for Atmospheric Research (NCAR)
[4]Savitribai Phule Pune University
[5]Indian Institute of Science Education and Research Mohali India
[6]National Center for Atmospheric Research (UCAR)
[7]Indian Institute of Tropical Meteorology, Pune
[8]Environment and Climate Change Canada
[9]Ministry of Earth Sciences

November 23, 2022

Abstract

This study investigates aerosol "sensitivity regimes" to explore the effectiveness of abating gaseous precursors to mitigate aerosols over the Indo-Gangetic Plain (IGP). A new mechanistic insight is proposed by integrating ISORROPIA-II thermodynamical model with high-resolution simultaneous measurements of precursor gases (HCl, HNO_3, and NH_3) and inorganic constituents of PM_1 and $PM_{2.5}$, monitored for the first time in India using MARGA-2S instrument. The estimated aerosol acidity (pH) of PM_1 and $PM_{2.5}$ was 4.49±0.53 and 4.58±0.48, respectively. The sensitivity of phase-partitioning (ε) of Cl^-, NO_3^-, and NH_4^+ to pH, ALWC, HCl, HNO_3, and NH_3 showed that fine aerosols fall in the "HCl and HNO_3 sensitive regime", emphasizing that HCl and HNO_3 reductions would be the most effective pathway to reduce aerosols in NH_3-rich IGP. Since existing mitigation strategies over IGP are random and ineffective, this novel insight is the first step in providing a thermodynamically consistent "roadmap" to mitigate aerosols effectively.

Hosted file

essoar.10511134.1.docx available at https://authorea.com/users/546417/articles/602403-abating-hcl-and-hno3-is-more-effective-than-nh3-for-mitigating-high-aerosol-loading-over-the-indo-gangetic-plain

Abating HCl and HNO_3 is more effective than NH_3 for mitigating high aerosol loading over the Indo-Gangetic Plain

Prodip Acharja[1,2], Sachin D. Ghude[1*], Baerbel Sinha[3*], Mary Barth[4], Rachana Kulkarni[2], Vinayak Sinha[3], Rajesh Kumar[4], Kaushar Ali[1], Gaurav Govardhan[1], Ismail Gultepe[5,6,7], Madhavan Nair Rajeevan[8]

[1]Indian Institute of Tropical Meteorology, Ministry of Earth Sciences, India

[2]Savitribai Phule Pune University, Pune, India 411007

[3]Department of Earth and Environmental Sciences, Indian Institute of Science Education and Research Mohali, Punjab, India

[4]National Center for Atmospheric Research, Boulder, CO, 80307, USA

[5]ECCC, Meteorological Research Division, Toronto, Ontario, Canada

[6]Ontario Technical University, Engineering and Applied Science, Oshawa, Ontario, Canada

[7]Istinye University, Faculty of Engineering, Istanbul, Turkey

[8]Ministry of Earth Science, Lodhi Road, New Delhi, India

Correspondence to:

Sachin D. Ghude

Email: `sachinghude@tropmet.res.in`;

Baerbel Sinha

Email: `bsinha@iisermohali.ac.in`

Abstract:

This study investigates aerosol "sensitivity regimes" to explore the effectiveness of abating gaseous precursors to mitigate aerosols over the Indo-Gangetic Plain (IGP). A new mechanistic insight is proposed by integrating ISORROPIA-II thermodynamical model with high-resolution simultaneous measurements of precursor gases (HCl, HNO_3, and NH_3) and inorganic constituents of PM_1 and $PM_{2.5}$, monitored for the first time in India using MARGA-2S instrument. The estimated aerosol acidity (pH) of PM_1 and $PM_{2.5}$ was 4.49±0.53 and 4.58±0.48, respectively. The sensitivity of phase-partitioning ( ) of Cl^-, NO_3^-, and NH_4^+ to pH, ALWC, HCl, HNO_3, and NH_3 showed that fine aerosols fall in the "HCl and HNO_3 sensitive regime", emphasizing that HCl and HNO_3 reductions would be the most effective pathway to reduce aerosols in NH_3-rich IGP. Since existing mitigation strategies over IGP are random and ineffective, this novel insight is the first step in providing a thermodynamically consistent "roadmap" to mitigate aerosols effectively.

Keywords: Gas-to-particle partitioning; Aerosol mitigation; Thermodynamics; ISORROPIA II; Aerosol acidity (pH) and aerosol liquid water content (ALWC); Indo-Gangetic Plain (IGP)

Plain Language Summary:

Researchers have a long-standing conundrum for the apparent disconnection between immense aerosol loading and adopted mitigation policies. We show that pollution mitigation cannot be achieved by "randomly" reducing the primary pollutants; instead, a thermodynamically consistent "roadmap" is needed. Indo-Gangetic Plain (IGP) experiences severe air pollution every winter, with ammonium chloride, ammonium nitrate as the major inorganic fractions of fine aerosols. Thermodynamic controls for the high aerosol loading show that fine aerosols fall in the "HCl and HNO_3 sensitive regime", and HCl and HNO_3 reductions would be the most effective pathway to reduce high aerosol loading. Though NH_3 mass concentration is much higher than HCl and HNO_3 but NH_3 reduction would not effectively mitigate aerosols. This new mechanistic insight suggests considering aerosol acidity (pH) and aerosol liquid water content (ALWC) more robustly and accurately as these parameters profoundly control the aerosol loading. Since existing aerosol mitigation strategies over IGP are random and ineffective, this novel analysis is the first step in providing "actionable intelligence" to the policymakers to abate precursors in a thermodynamically consistent way, like those for Europe, the USA, and other climatic regions.

1. Introduction

Air pollution is a major cause of millions of premature deaths around the world (Cohen et al., 2015). Mitigating high aerosol loading is a major concern for researchers over the globe. But to regulate or mitigate something, it needs to be measured, monitored, and investigated thoroughly, but despite unprecedented efforts, the understanding of the intricate physical, chemical, and thermodynamical properties of atmospheric constituents has remained something of a mystery (Seinfeld and Pandis, 1997; Guo et al., 2018; Gultepe et al., 2007; Nenes et al., 2020).

Indo Gangetic Plain (IGP) is documented to be one of the most polluted regions in the world (WHO, 2016; Ravishankara et al., 2020). There is a growing need to abate high aerosol loading in IGP, as it severely affects the ecosystem and human health (Ghude et al., 2017; Sinha et al., 2019). During wintertime, the mass loading of PM_1, $PM_{2.5}$ generally exceeds 400-600 µg m^{-3}, which causes severe negative impacts on human health and the ecosystem. These fine aerosols are primarily composed of chloride, sulfate, nitrate, and ammonium (CSNA) in the IGP (Acharja et al., 2020). The observed hourly chloride concentrations sometimes exceeded 100 µg m^{-3}, considered to be among the highest reported anywhere in the world. The gas-phase ammonia (NH_3) was also found to be very high, which significantly affects the secondary aerosol formation in winter (Acharja et al., 2021). Extensive effort is needed to improve our scientific understanding, to regulate aerosol loading effectively. Several recent studies have

investigated the sensitivity of aerosols to the reduction in precursor gases over China, USA, and Europe (Nenes et al., 2020; Guo et al., 2018), but studies conducted over India remain elusive to date.

This study aims to provide new mechanistic insights into aerosol mitigation by integrating the dataset of precursor gases (HCl, HNO_3, and NH_3) and inorganic constituents (Cl^-, NO_3^-, SO_4^{2-}, Na^+, NH_4^+, K^+, Ca^{2+}, and Mg^{2+}) of PM_1 and $PM_{2.5}$ acquired using the first deployment of the MARGA-2S instrument in IGP with the ISORROPIA-II thermodynamic equilibrium model simulations. The dataset filled the much-needed data gap for quantitative analysis and provided the best opportunity to investigate aerosol sensitivity to precursors over IGP. We explored a "thermodynamical framework" to show that aerosol mitigation cannot be achieved by "randomly" reducing the primary pollutants, rather a fundamental understanding of complex thermodynamical control of aerosol loading is needed. For this, we determined pH and ALWC using the ISORROPIA-II thermodynamic equilibrium model. The accuracy of the model simulation is checked by comparing the model predicted species concentrations with MARGA-2S observations. After verifying the reliability of the model prediction, the sensitivity of gas-to-particle partitioning of major aerosol species like chloride, nitrate, and ammonium to pH and ALWC is checked using the sigmoidal (S) curves. Finally, we investigated the sensitivity of gaseous precursors like HCl, HNO_3, and NH_3 to the formation of fine particulate matter to explore the aerosol "sensitivity regimes" and establish a thermodynamically consistent framework for effective aerosol mitigation.

2. Materials and Methods

2.1 Sensitivity of aerosol mass loading to pH, ALWC using sigmoidal (S) curves

Factors that profoundly influence almost every aspect of aerosols are aerosol acidity (pH) and aerosol liquid water content (ALWC) (Weber et al., 2016; Nenes et al., 1999). The direct monitoring of aerosol pH is highly challenging since an established analytical method of directly determining aerosol pH does not exist. Previous studies used several proxy methods like H^+ ion concentration, ion balance, ammonium-to-sulfate ratio, and cation-to-anion ratio to indirectly infer the fine particle pH (Toon et al., 1986; Rindelaub et al., 2016). Pye et al. (2020) showed that these methods could not estimate aerosol acidity accurately, and a small bias in estimated pH may cause substantial errors in the chemical and thermodynamical properties of aerosols (Hennigan et al., 2015). To accurately estimate pH and ALWC, numerous studies have used thermodynamic models like E-AIM, MARS, EQUISOLV, and ISORROPIA-II, among which ISORROPIA-II is the most used that can predict pH and ALWC with great accuracy (Fountoukis and Nenes 2007; Nenes et al., 1999; Pye et al., 2020).

The sensitivity of the phase partitioning of nitrate [(NO_3^-)], chloride [(Cl^-)] and ammonium [(NH_4^+)] to pH, ALWC, and T is estimated using the Henry's law constant (Pitzer et al., 1973; Clegg et al., 1998; Meissner et a., 1972) and

following the methodology given in Guo et al., (2016) as

$$\varepsilon\left(\mathrm{NO}_3^-\right) = \frac{H^*_{\mathrm{HNO}_3}\ \mathrm{R\ T\ ALWC}_i \times 0.987\ \times 10^{-14}}{\gamma_{H^+}\gamma_{\mathrm{NO}_3^-}10^{-pH} +\ H^*_{\mathrm{NO}_3}\ \mathrm{R\ T\ ALWC}_i \times 0.987\ \times 10^{-14}} \tag{1}$$

$$\varepsilon\left(\mathrm{Cl}^-\right) = \frac{H^*_{\mathrm{HCl}}\ \mathrm{R\ T\ ALWC}_i \times 0.987\ \times 10^{-14}}{\gamma_{H^+}\gamma_{\mathrm{Cl}^-}10^{-pH} +\ H^*_{\mathrm{HCl}}\ \mathrm{R\ T\ ALWC}_i \times 0.987\ \times 10^{-14}} \tag{2}$$

and

$$\varepsilon\left(\mathrm{NH}_4^+\right) = \frac{\frac{\gamma_{H^+}\ 10^{-pH}}{\gamma_{\mathrm{NH}_4^+}}\ H^*_{\mathrm{NH}_3}\ \mathrm{R\ T\ ALWC}_i \times 0.987\ \times 10^{-14}}{1 + \frac{\gamma_{H^+}\ 10^{-pH}}{\gamma_{\mathrm{NH}_4^+}}\ H^*_{\mathrm{NH}_3}\ \mathrm{R\ T\ ALWC}_i \times 0.987\ \times 10^{-14}}\ , \tag{3}$$

where is the activity coefficient of protonated species in the aqueous medium. H^* is the equilibrium constants of HNO_3, HCl, and NH_3 adopted from Clegg and Brimblecombe (1989), and Clegg (1998). Then, the units were converted from mole fraction-based unit atm^{-1} to molality-based unit $mole^2\ kg^{-2}\ atm^{-1}$ (Nenes et al., 1999; Patwardhan et al., 1986). R is the universal gas constant (8.314 J $K^{-1}\ mol^{-1}$), and the value 0.987 is for the transformation of 1 atm to 1 bar. The equations describe the HNO_3-NO_3^-, NH_3-NH_4^+, and HCl-Cl^- partitioning and the estimated values of $ALWC_i$ and T were used to evaluate the sigmoidal (S) curves of (NO_3^-), (Cl^-), and (NH_4^+) at different pH regimes.

2.2 Sensitivity of aerosols to HCl, HNO_3, and NH_3 perturbations and aerosol "sensitivity regimes"

The estimated pH and ALWC of PM_1 and $PM_{2.5}$ were used as coordinates to represent aerosols in different "sensitivity regimes" where aerosol mass is sensitive to HNO_3, HCl, and/or NH_3 variability (Nenes et al., 2020). Three parameters Ψ, Ω, and are defined as:

$$\Psi = \frac{H^*_{H\mathrm{NO}_3}\ R\ T\ \times 0.987\ \times 10^{-14}}{\gamma_{H^+}\gamma_{\mathrm{NO}_3^-}} \tag{4}$$

$$\Omega\ = \frac{H^*_{\mathrm{HCl}}\ R\ T\ \times 0.987\ \times 10^{-14}}{\gamma_{H^+}\gamma_{\mathrm{Cl}^-}} \tag{5}$$

$$\varphi = \frac{\gamma_{H^+}}{\gamma_{\mathrm{NH}_4^+}}\ H^*_{\mathrm{NH}_3}\ R\ T\ \times 0.987\ \times 10^{-14} \tag{6}$$

Substituting these three parameters in equations 1 - 3, the partitioning ratio of (NO_3^-), (Cl^-) and (NH_4^+) can be expressed as a function of ALWC, like

$$\varepsilon\,(\mathrm{NO}_3^-) = \frac{\Psi \;\times\; \mathrm{ALWC}_i}{[H^+] + \;\Psi \times\; \mathrm{ALWC}_i}\;, \tag{7}$$

$$\varepsilon\,(\mathrm{Cl}^-) = \frac{\Omega \;\times\; \mathrm{ALWC}_i}{[H^+] + \;\Omega \times\; \mathrm{ALWC}_i}\;, \tag{8}$$

and

$$\varepsilon\left(\mathrm{NH}_4^+\right) = \frac{\varphi \;\times [H^+] \;\times\; \mathrm{ALWC}_i}{1 + \;\varphi \times\; [H^+] \;\times\; \mathrm{ALWC}_i}\quad . \tag{9}$$

To check the sensitivity of these partitioning fractions to aerosol pH and ALWC, we assume a characteristic partitioning ratio ( ) value of 0.1, and define the threshold value of (NO_3^-), (Cl^-) and (NH_4^+) as , , and , and they are respectively given as

$$\alpha = \frac{\Psi \;\times\; \mathrm{ALWC}_i}{[H^+] + \;\Psi \times\; \mathrm{ALWC}_i}\quad , \tag{10}$$

$$\beta = \frac{\Omega \;\times [H^+] \;\times\; \mathrm{ALWC}_i}{1 + \;\Omega \times\; [H^+] \;\times\; \mathrm{ALWC}_i}\quad , \tag{11}$$

and

$$\gamma = \frac{\varphi \;\times [H^+] \;\times\; \mathrm{ALWC}_i}{1 + \;\varphi \times\; [H^+] \;\times\; \mathrm{ALWC}_i}\quad . \tag{12}$$

Above the threshold value (= 10%) the PM_1, $PM_{2.5}$ aerosols are sensitive to HNO_3, HCl, or NH_3 emissions. Based on these "characteristic" threshold values, we define "characteristic acidity" for nitrate, (pH'), chloride (pH") and ammonium (pH"'), respectively, as

$$pH' = -\log\,[(\frac{1-\alpha}{\quad})\;\Psi \times \mathrm{ALWC}_i], \tag{13}$$

$pH'' = \log\ [(\frac{1-\beta}{})\ \varphi\ \times \mathrm{ALWC}_i]$, (14)

and

$pH''' = \log\ [(\frac{1-\gamma}{})\ \Omega \times \mathrm{ALWC}_i]$, (15)

which vary logarithmically only function of $\mathrm{ALWC_i}$. Using these characteristic values as coordinates, six "sensitivity regimes" are defined as

- Regime I: pH < pH', pH" and pH > pH"', where aerosol is not sensitive to HNO_3, HCl or NH_3 change and defined as "insensitive",
- Regime II: pH > pH', pH < pH" and pH > pH"', where aerosol is sensitive to HNO_3 and not sensitive to HCl and NH_3 perturbations and defined as "HNO_3 sensitive",
- Regime III: pH > pH', pH" and pH > pH"', where aerosol is sensitive to HCl, HNO_3 and not sensitive to NH_3 perturbations and defined as "HCl and HNO_3 sensitive",
- Regime IV: pH > pH', pH" and pH < pH'", where aerosol is sensitive to HCl, $HNO_{3,}$ and NH_3 perturbations and defined as "HCl, NH_3 and HNO_3 sensitive",
- Regime V: pH > pH' and pH < pH", pH'", where aerosol is sensitive to HNO_3 and NH_3 and not sensitive to HCl and defined as "HNO_3 and NH_3 sensitive", and
- Regime VI: pH < pH', pH" and pH < pH'", where aerosol is sensitive to NH_3 and not sensitive to HCl and HNO_3 and defined as "NH_3 sensitive".

3. Results

3.1 Evaluation of ISORROPIA-II thermodynamical model simulations

Running a thermodynamical equilibrium model like ISORROPIA-II to predict pH and ALWC is not necessarily straightforward and is comparatively new to the atmospheric science community in India. The ISORROPIA-II model was run in the "forward" mode using the hourly measured total (gas + particle) species concentrations instead of only particle-phase concentrations as input (Hennigan et al., 2015). This mode is considered to be more accurate, and the predicted data is thoroughly checked and compared to MARGA-2S measurements to validate the model simulations.

Figure 1 shows the comparison between the predicted and measured concentrations of NH_4^+, NO_3^-, Cl^- of PM_1 and $PM_{2\cdot5}$. The predicted PM_1 NH_4^+ (r =0.97), NO_3^- (r = 0.93), Cl^- (r = 0.98) and $PM_{2.5}$ NH_4^+ (r =0.87), NO_3^- (r = 0.98), Cl^- (r = 0.99) showed very good correlation with the measured concentrations. Along with these particle-phase species, the predicted and measured gas-phase NH_3 (r = 0.93) and gas-to-particle partitioning ratio ( ) of ammonium

(NH_4^+) (r = 0.90) also correlated well. The normalized mean bias (NMB) between the measured and predicted NH_4^+, NO_3-, Cl^-, and NH_3 concentrations was very low (10%). These high correlations were attributed to the reliability of the ISORROPIA-II model simulations.

3.2 Temporal variation of pH and ALWC of PM_1 and $PM_{2.5}$

The pH and ALWC of PM_1 and $PM_{2.5}$ were estimated during 19 December 2017 to 10 February 2018. The predicted pH of PM_1 varied between 2.19 to 5.63, and the mean PM_1 pH (average±SD) was 4.49±0.53. The $PM_{2.5}$ pH ranged between 2.55 to 6.54 with a mean value of 4.58±0.48. The predicted pH of $PM_{2.5}$ was similar to the measured $PM_{2.5}$ pH of 4.6±0.5 over Delhi, estimated during the WiFEX campaign period of 2015-16, showing the reliability and accuracy of the ISORROPIA-II model simulation (Ali et al., 2019). The accuracy of ISORROPIA-II thermodynamic model simulations is crucial, as most chemical transport models often underestimate aerosol acidity (Nault et al., 2021).

As liquid water makes up a significant part of the aerosol volume, the temporal variation of ALWC was investigated. The mean ALWC of PM_1 and $PM_{2.5}$ was 169±205 and 324±393 µg m^{-3}, respectively, showing that higher ALWC corresponds to higher PM concentrations. This is evident from Henry's law, which shows that particles with high ALWC would take up more gaseous pollutants, and the equilibrium would lead to an increase in their water content and the formation of more secondary aerosol.

The ALWC variability generally controlled the pH variability. The lesser ALWC of PM_1 caused it to be slightly more acidic than $PM_{2.5}$, as H^+ gets more diluted in higher liquid water in $PM_{2.5}$. The aerosol liquid water serves as a reaction medium and enhances the chemical reaction rates of heterogeneous, multiphase reactions, and the multiphase reactions inside aerosol water are much faster than heterogeneous reactions on the solid surface (Ravishankara et al., 1997; Hanson et al., 1994; Rood et al., 1989). This implies the crucial role of pH and ALWC in high aerosol loading.

3.3 Gas-to-particle phase partitioning of aerosols during winter over IGP

The average chloride partitioning ratio (Cl^-) of PM_1 and $PM_{2.5}$ was 0.93±0.09 and 0.96±0.07 respectively, implying the dominant presence of chloride in the particle-phase during winter. The (Cl^-) was 0.4 at RH 50%, and at RH 80%, the (Cl^-) sharply increased to 0.95, showing the enhanced chloride formation in the particle-phase. The increased phase-partitioning of total chloride (HCl + Cl^-) at high humid conditions can further promote chloride formation caused by increased ALWC. The enhanced ALWC increases pH by dilution, further increasing total chloride partitioning and significantly increasing PM_1, $PM_{2.5}$ chloride in a positive feedback loop (Guo et al., 2018; Song et al., 2018).

The average (NO_3^-) of PM_1 and $PM_{2.5}$ was 0.83±0.11 and 0.89±0.08 respectively. This shows the dominance of particle-phase nitrate over gas-phase HNO_3

during winter. The high particle-phase nitrate concentrations significantly impact the total aerosol loading as the presence of more ammonium nitrate reduces the mutual deliquescence relative humidity (MDRH) of aerosols resulting in the formation of more secondary aerosols in polluted conditions (Davis et al., 2015; Shi et al., 2017; Nah et al., 2018). When the ammonium nitrate concentration is high, especially in humid and ammonia-rich conditions, it could promote secondary aerosol formation through uptake kinetic regime and changing the particle state (Liu et al., 2021). So, it is crucial to investigate the sensitivity of (NO_3^-) to factors like pH, ALWC, and HNO_3 following the Eq 1.

Interestingly, ammonium (NH_4^+) phase partitioning showed the opposite behavior to chloride and nitrate. Not the particle-phase ammonium (NH_4^+), but the gas-phase ammonia (NH_3) dominated, and the average (NH_4^+) was 0.42±0.17, 0.55±0.15 for PM_1, $PM_{2.5}$ respectively. This abundant gas-phase ammonia plays a crucial role in developing high ammonium salts loading (Acharja et al., 2021). Thermodynamically, ammonia neutralizes the atmospheric acids like HCl, H_2SO_4, and HNO_3 based on the order of solubility, and as HCl is the strongest acid, NH_3 first reacts with HCl to form NH_4Cl. Then the excess NH_3 reacts with H_2SO_4 over highly volatile HNO_3, forming $(NH_4)_2SO_4$ first and then NH_4NO_3 (Dentener and Crutzen 1994; Collett et al., 1994; Toon et al., 1986; Nemitz et al., 2004). However, it is crucial to note that the PM_1 and $PM_{2.5}$ were moderately acidic despite the ammonia-rich atmosphere, depicting the weak sensitivity of pH to ammonia and the significance of complex thermodynamic control on aerosol loading.

3.4 Sensitivity of gas-to-particle partitioning ( ) to pH and ALWC using sigmoidal (S) curves

Figures 2a, 2b shows the variability of (Cl^-), (NO_3^-) with pH, ALWC, and T. Three prominent regimes are shown, in which varies between complete gas-phase (~0%) to complete particle-phase (~100%). In regime 1, (Cl^-), (NO_3^-) asymptotically approaches 0, and the total species primarily remain in the gas-phase. In regime 3, asymptotically approaches 1, and the whole species is in the particle phase. In regime 2, varies between 0 and 1, and the species remain as a mixture of gas and particle-phase. Modulating this "pH window" the particle-phase can be shifted to gas-phase resulting in less particle-phase loading in the atmosphere. pH_{50} is defined, where (Cl^-) and (NO_3^-) is 0.5 and total chloride, nitrate remained 50% in the gas-phase and 50% in the particle-phase. Modulating the phase partitioning ratio ( ) to $_{(pH50)}$ value, the particle-phase loading of chloride and nitrate can be reduced to 50%. Figures 2a, 2b shows that a pH change from 4.45 to 2.4 and 4.45 to 1.9 is required to reduce (Cl^-) and (NO_3^-) to 50%. The variability in at a constant pH is caused by the variation in ALWC, implying the significance of ALWC in modulating the particle-phase fraction.

In Figures 2c and 2d, we have included the variability of ammonium (NH_4^+) phase partitioning along with chloride (Cl^-) and nitrate (NO_3^-). The sigmoidal (S) curves show that the particle-phase chloride and nitrate increase with pH,

whereas ammonium decreases. This inverse relation of ammonium compared to chloride and nitrate is due to opposite acid and base partitioning responses to pH and needs to be considered to develop effective abatement measures. We estimated the sensitivity and effectiveness of phase-partitioning to precursors like HCl, HNO_3, and NH_3 and defined "sensitivity regimes" in different colors.

In the blue regime, a marginal change in HCl and HNO_3 would significantly shift the particle-phase fraction of (Cl^-), (NO_3^-). We defined this regime as "HCl and HNO_3 sensitive regime", where ammonia remains almost exclusively in the gas-phase, and perturbation in NH_3 concentrations would not change the ammonium particle-phase fraction regardless of the level of total ammonia present. So the "HCl and HNO_3 sensitive regime" is also an "NH_3 insensitive regime". A fractional change in NH_3 concentrations would significantly change (NH_4^+) in the pink regime, and we termed it the "NH_3 sensitive regime". In the mid-range of the sigmoidal curves, a small perturbation in the HCl, HNO_3, and NH_3 concentrations would directly impact the particle-phase loading of chloride, nitrate, and ammonium and defined as the "HCl, HNO_3, and NH_3 sensitive regime".

The estimated pH of PM_1 and $PM_{2.5}$ falls in regime 3, on the flat side of the S curves. Here, two possibilities emerge as the pathway to modulate high aerosol concentrations. First, a substantial reduction in pH is needed, which would evaporate NH_4Cl and NH_4NO_3 and shift them to the gas-phase, which may not be feasible due to the health and environmental implications of high aerosol acidity. Second, reducing HCl and HNO_3 concentrations would most effectively reduce particle-phase loading as aerosols are in the "HCl, HNO_3 sensitive regime". This pathway is feasible compared to the other, and we conclude that HCl and HNO_3 controlling policy should be adopted to reduce aerosol loading in the IGP.

3.5 Aerosol mass loading sensitivity to HCl, HNO_3, and NH_3 perturbations

We explored a mathematical framework to reduce ammonium chloride and ammonium nitrate concentrations by following the methodology of Nenes et al., (2020). Using pH and ALWC as coordinates, we defined six "sensitivity regimes", where aerosols are sensitive to HCl, HNO_3, and NH_3 perturbations. As chloride dominates the inorganic mass fraction of fine aerosol in the IGP, we rigorously investigated the aerosol mass sensitivity to HCl emissions and defined the "HCl sensitive regime" for the first time. This is significantly different from studies conducted over China, Europe, and USA, where researchers have investigated aerosol sensitivity to only HNO_3 and NH_3 and did not investigate the "HCl sensitive regime".

The "sensitivity regimes" are shown in different colors in Figure 3. 1100 hourly observational data points are plotted to check the instantaneous response of aerosol loading to HCl, HNO_3, and NH_3 variability. Figures 3a and 3c show PM_1 and $PM_{2.5}$ aerosols to remain in the pink shaded region, where aerosols respond proportionally to changes in the HCl and HNO_3 emissions but tend

to be insensitive to NH_3 emissions. We defined the pink regime as "HCl and HNO_3 sensitive regime", indicating that HCl and HNO_3 reduction would be the most effective pathway in controlling aerosol pollution over IGP. Ammonia is much higher than HCl and HNO_3 in IGP, but fine aerosols are not sensitive to variations of it. Instead, HCl and HNO_3 are by far the limiting factors in aerosol loading, which should be controlled by controlling the major HCl and NO_x emissions over IGP.

In Figures 3b and 3d, all the data points are color-coded with PM_1 and $PM_{2.5}$ concentrations respectively. The figures demonstrate that higher aerosol loading is often associated with higher ALWC in the "HCl and HNO_3 sensitive regime". Interestingly, the ALWC usually ranges between tens to hundreds of micrograms per cubic meter in climatic regions like China and USA, but over IGP the ALWC is an order of magnitude higher, sometimes reaching ~2000-2500 µg m^{-3} for PM_1 and $PM_{2.5}$. This acidic aerosol liquid water significantly influences the phase-partitioning and demonstrates the impact of pH and ALWC on aerosol loading. Fewer cases with low PM_1, $PM_{2.5}$ levels were found in the NH_3 sensitive regime, showing the less importance of NH_3 abatement to modulate high aerosol loading. It is also interesting to note that a significant reduction in NH_3 emissions may affect agricultural productivity and potentially increase aerosol acidity. So the HCl and HNO_3 reductions should be adopted to mitigate aerosols most effectively.

4. Discussion

The complex interaction of intricate physical, chemical, and thermodynamical processes influencing the aerosol loading is schematically shown in Figure 4. Two different atmospheric scenarios are characterized: clean atmosphere and polluted atmosphere, where photochemistry plays a distinct role during the clean period, and multiphase, heterogeneous chemistry dominates the pollution episodes, as the homogeneous gas-phase reactions were suppressed due to reduced solar radiation. As schematically shown, the acidic gases are first absorbed on the surface layer of aerosols, and heterogeneous reactions rapidly occur at the surface resulting in the rapid increase in secondary aerosols concentrations. The newly formed particles then get dispersed through the liquid phase in high ALWC, where multiphase reactions govern. The higher surface-area-to-volume ratio of PM_1 than $PM_{2.5}$ suggests the heterogeneous chemistry in PM_1 to be more crucial than $PM_{2.5}$.

From a thermodynamic perspective, the equilibrium of phase-partitioning is governed by the complex interplay between chemical composition and parameters like pH, ALWC, and T. We show that there are two fundamental ways to modulate semi-volatile species like ammonium chloride and ammonium nitrate, (i) either by controlling the emissions of precursors HCl, HNO_3, and NH_3 or (ii) by moving the chloride, nitrate, and ammonium out of the particle-phase and shifting to the gas-phase. The explored "sensitivity regimes" of PM_1 and $PM_{2.5}$ show that abating HCl and HNO_3 is more effective than NH_3 for mitigating high aerosol loading over the IGP.

A recent study conducted in Europe and USA suggested that ammonia reduction would be the most effective pathway to reduce aerosol loading as it is more cost-effective than NO_x reduction (Gu et al., 2021). But, this study shows that the sensitivity and effectiveness of the adopted reduction mechanisms are more crucial than the cost-effectiveness. If aerosols are not sensitive to the reductions of a specific precursor, then the cost-effectiveness would not assist in developing an effective mitigation policy. Rather, the thermodynamically consistent sensitivity analysis would effectively address the outstanding air pollution mitigation problem, as evidenced by this study.

5. Conclusions

After a long-standing quest for an effective aerosol mitigation framework, here we present the first thermodynamically consistent "roadmap" over the Indo-Gangetic Plain (IGP) to effectively mitigate aerosols. The proposed framework categorically considers aerosol acidity (pH) and aerosol liquid water content (ALWC) as the crucial parameters and investigates the effectiveness of gaseous precursor reductions in aerosol mitigation. Six "sensitivity regimes" are defined as (a) "HNO_3 sensitive", (b) "HCl and HNO_3 sensitive", (c) "HCl, NH_3 and HNO_3 sensitive", (d) "HNO_3 and NH_3 sensitive", (e) "NH_3 sensitive", and (f) "insensitive" to explore the sensitivity of gaseous precursors in the formation of fine aerosols. The application of the framework to the observational dataset shows PM_1 and $PM_{2.5}$ aerosols to fall in the "HCl and HNO_3 sensitive regime", emphasizing that HCl and HNO_3 reductions would be the most effective pathway to reduce aerosol loading over IGP. The thermodynamic control suggests that although NH_3 is much higher than HCl and HNO_3, but NH_3 reduction should not be explicitly prioritized to mitigate aerosols. This is in disparity with the existing aerosol mitigation strategies over IGP, which are mostly ineffective and not thermodynamically favorable. This novel insight provides "actionable intelligence" to the policymakers to abate precursors not at "random" but in a thermodynamically consistent way.

Acknowledgments

The Indian Institute of Tropical Meteorology (IITM) is funded by the Ministry of Earth Sciences (MoES), Government of India. We thank the Director, IITM, for his continuous support and encouragement. The authors are grateful to the Ministry of Earth Sciences, Government of India, for support throughout the Winter Fog Experiment (WiFEX) field campaign. The lead author's fellowship was supported by the National Supercomputing Mission (NSM) program grant at C-DAC, and we are grateful to the Executive Director and the Director-General of C-DAC.

Open Research

The data used to prepare this manuscript can be found in the link: https://osf.io/6HGS7/.

References:

Acharja, P., Ali, K., Ghude, S.D., Sinha, V., Sinha, B., Kulkarni, R., Gultepe, I. and Rajeevan, M.N., 2021. Enhanced secondary aerosol formation driven by excess ammonia during fog episodes in Delhi, India. Chemosphere, p.133155.

Acharja, P., Ali, K., Trivedi, D.K., Safai, P.D., Ghude, S., Prabhakaran, T. and Rajeevan, M., 2020. Characterization of atmospheric trace gases and water soluble inorganic chemical ions of PM1 and PM2. 5 at Indira Gandhi International Airport, New Delhi during 2017–18 winter. Science of the Total Environment, 729, p.138800.

Ali, K., Acharja, P., Trivedi, D.K., Kulkarni, R., Pithani, P., Safai, P.D., Chate, D.M., Ghude, S., Jenamani, R.K. and Rajeevan, M., 2019. Characterization and source identification of PM2. 5 and its chemical and carbonaceous constituents during Winter Fog Experiment 2015–16 at Indira Gandhi International Airport, Delhi. Science of The Total Environment, 662, pp.687-696.

Barth, M.C., Rasch, P.J., Kiehl, J.T., Benkovitz, C.M. and Schwartz, S.E., 2000. Sulfur chemistry in the National Center for Atmospheric Research Community Climate Model: Description, evaluation, features, and sensitivity to aqueous chemistry. Journal of Geophysical Research: Atmospheres, 105(D1), pp.1387-1415

Bian, Y.X., Zhao, C.S., Ma, N., Chen, J. and Xu, W.Y., 2014. A study of aerosol liquid water content based on hygroscopicity measurements at high relative humidity in the North China Plain. Atmospheric Chemistry and Physics, 14(12), pp.6417-6426.

Bougiatioti, A., Nikolaou, P., Stavroulas, I., Kouvarakis, G., Weber, R., Nenes, A., Kanakidou, M. and Mihalopoulos, N., 2016. Particle water and pH in the eastern Mediterranean: source variability and implications for nutrient availability. Atmospheric Chemistry and Physics, 16(7), pp.4579-4591.

Clegg, S.L. and Brimblecombe, P., 1989. Solubility of ammonia in pure aqueous and multicomponent solutions. The Journal of Physical Chemistry, 93(20), pp.7237-7248.

Clegg, S.L., Brimblecombe, P. and Wexler, A.S., 1998. Thermodynamic model of the system H+− NH4+− SO42-− NO3-− H2O at tropospheric temperatures. The Journal of Physical Chemistry A, 102(12), pp.2137-2154.

Cohen, A.J., Brauer, M., Burnett, R., Anderson, H.R., Frostad, J., Estep, K., Balakrishnan, K., Brunekreef, B., Dandona, L., Dandona, R. and Feigin, V., 2017. Estimates and 25-year trends of the global burden of disease attributable to ambient air pollution: an analysis of data from the Global Burden of Diseases Study 2015. The Lancet, 389(10082), pp.1907-1918.

Collett Jr, J.L., Bator, A., Rao, X. and Demoz, B.B., 1994. Acidity variations across the cloud drop size spectrum and their influence on rates of atmospheric sulfate production. Geophysical Research Letters, 21(22), pp.2393-2396.

Davis, R.D., Lance, S., Gordon, J.A., Ushijima, S.B. and Tolbert, M.A., 2015. Contact efflorescence as a pathway for crystallization of atmospherically relevant particles. Proceedings of the National Academy of Sciences, 112(52), pp.15815-15820.

Dentener, F. J. and Crutzen, P. J.: A three-dimensional model of the global ammonia cycle, J. Atmos. Chem., 19, 331–369, https://doi.org/10.1007/BF00694492, 1994.

Fountoukis, C. and Nenes, A., 2007. ISORROPIA II: a computationally efficient thermodynamic equilibrium model for K+–Ca 2+–Mg 2+–NH 4+–Na+–SO 4 2−–NO 3−–Cl−–H 2 O aerosols. Atmospheric Chemistry and Physics, 7(17), pp.4639-4659.

Ghude, S.D., Bhat, G.S., Prabhakaran, T., Jenamani, R.K., Chate, D.M., Safai, P.D., Karipot, A.K., Konwar, M., Pithani, P., Sinha, V. and Rao, P.S.P., 2017. Winter fog experiment over the Indo-Gangetic plains of India. Current Science, pp.767-784.

Gu, B., Zhang, L., Van Dingenen, R., Vieno, M., Van Grinsven, H.J., Zhang, X., Zhang, S., Chen, Y., Wang, S., Ren, C. and Rao, S., 2021. Abating ammonia is more cost-effective than nitrogen oxides for mitigating PM2. 5 air pollution. Science, 374(6568), pp.758-762.

Gultepe, I., Tardif, R., Michaelides, S.C., Cermak, J., Bott, A., Bendix, J., Müller, M.D., Pagowski, M., Hansen, B., Ellrod, G. and Jacobs, W., 2007. Fog research: A review of past achievements and future perspectives. Pure and applied geophysics, 164(6), pp.1121-1159.

Guo, H., Otjes, R., Schlag, P., Kiendler-Scharr, A., Nenes, A. and Weber, R.J., 2018. Effectiveness of ammonia reduction on control of fine particle nitrate. Atmospheric Chemistry and Physics, 18(16), pp.12241-12256.

Guo, H., Xu, L., Bougiatioti, A., Cerully, K.M., Capps, S.L., Hite Jr, J.R., Carlton, A.G., Lee, S.H., Bergin, M.H., Ng, N.L. and Nenes, A., 2015. Fine-particle water and pH in the southeastern United States. Atmospheric Chemistry and Physics, 15(9), pp.5211-5228.

Hanson, D.R., Ravishankara, A.R. and Solomon, S., 1994. Heterogeneous reactions in sulfuric acid aerosols: A framework for model calculations. Journal of Geophysical Research: Atmospheres, 99(D2), pp.3615-3629.

Hennigan, C.J., Izumi, J., Sullivan, A.P., Weber, R.J. and Nenes, A., 2015. A critical evaluation of proxy methods used to estimate the acidity of atmospheric particles. Atmospheric Chemistry and Physics, 15(5), pp.2775-2790.

Kumar, R., Barth, M.C., Pfister, G.G., Delle Monache, L., Lamarque, J.F., Archer-Nicholls, S., Tilmes, S., Ghude, S.D., Wiedinmyer, C., Naja, M. and Walters, S., 2018. How will air quality change in South Asia by 2050?. Journal of Geophysical Research: Atmospheres, 123(3), pp.1840-1864.

Liu, M., Song, Y., Zhou, T., Xu, Z., Yan, C., Zheng, M., Wu, Z., Hu, M., Wu, Y. and Zhu, T., 2017. Fine particle pH during severe haze episodes in northern China. Geophysical Research Letters, 44(10), pp.5213-5221.

Liu, Y., Feng, Z., Zheng, F., Bao, X., Liu, P., Ge, Y., Zhao, Y., Jiang, T., Liao, Y., Zhang, Y. and Fan, X., 2021. Ammonium nitrate promotes sulfate formation through uptake kinetic regime. Atmospheric Chemistry and Physics Discussions, pp.1-39.

Malm, W.C. and Day, D.E., 2001. Estimates of aerosol species scattering characteristics as a function of relative humidity. Atmospheric Environment, 35(16), pp.2845-2860.

Meissner, H.P. and Tester, J.W., 1972. Activity coefficients of strong electrolytes in aqueous solutions. Industrial & Engineering Chemistry Process Design and Development, 11(1), pp.128-133.

Nah, T., Guo, H., Sullivan, A.P., Chen, Y., Tanner, D.J., Nenes, A., Russell, A., Ng, N.L., Huey, L.G. and Weber, R.J., 2018. Characterization of aerosol composition, aerosol acidity, and organic acid partitioning at an agriculturally intensive rural southeastern US site. Atmospheric Chemistry and Physics, 18(15), pp.11471-11491.

Nault, B.A., Campuzano-Jost, P., Day, D.A., Jo, D.S., Schroder, J.C., Allen, H.M., Bahreini, R., Bian, H., Blake, D.R., Chin, M. and Clegg, S.L., 2021. Chemical transport models often underestimate inorganic aerosol acidity in remote regions of the atmosphere. Communications Earth & Environment, 2(1), pp.1-13.

Nemitz, E., Sutton, M.A., Wyers, G.P. and Jongejan, P.A.C., 2004. Gas-particle interactions above a Dutch heathland: I. Surface exchange fluxes of NH 3, SO 2, HNO 3 and HCl. Atmospheric Chemistry and Physics, 4(4), pp.989-1005.

Nenes, A., Pandis, S.N. and Pilinis, C., 1999. Continued development and testing of a new thermodynamic aerosol module for urban and regional air quality models. Atmospheric Environment, 33(10), pp.1553-1560.

Nenes, A., Pandis, S.N., Kanakidou, M., Russell, A., Song, S., Vasilakos, P. and Weber, R.J., 2020. Aerosol acidity and liquid water content regulate the dry deposition of inorganic reactive nitrogen. Atmos. Chem. Phys. Discuss, 10.

Pathak, R.K., Louie, P.K. and Chan, C.K., 2004. Characteristics of aerosol acidity in Hong Kong. Atmospheric Environment, 38(19), pp.2965-2974.

Patwardhan, V.S. and Kumar, A., 1986. A unified approach for prediction of thermodynamic properties of aqueous mixed-electrolyte solutions. Part I: Vapor pressure and heat of vaporization. AIChE journal, 32(9), pp.1419-1428.

Parworth, C.L., Young, D.E., Kim, H., Zhang, X., Cappa, C.D., Collier, S. and Zhang, Q., 2017. Wintertime water-soluble aerosol composition and particle

water content in Fresno, California. Journal of Geophysical Research: Atmospheres, 122(5), pp.3155-3170.

Pitzer, K.S. and Mayorga, G., 1973. Thermodynamics of electrolytes. II. Activity and osmotic coefficients for strong electrolytes with one or both ions univalent. The Journal of Physical Chemistry, 77(19), pp.2300-2308.

Pye, H.O., Nenes, A., Alexander, B., Ault, A.P., Barth, M.C., Clegg, S.L., Collett Jr, J.L., Fahey, K.M., Hennigan, C.J., Herrmann, H. and Kanakidou, M., 2020. The acidity of atmospheric particles and clouds. Atmospheric chemistry and physics, 20(8), pp.4809-4888.

Ravishankara, A.R., 1997. Heterogeneous and multiphase chemistry in the troposphere. Science, 276(5315), pp.1058-1065.

Ravishankara, A.R., David, L.M., Pierce, J.R. and Venkataraman, C., 2020. Outdoor air pollution in India is not only an urban problem. Proceedings of the National Academy of Sciences, 117(46), pp.28640-28644.

Rindelaub, J.D., Craig, R.L., Nandy, L., Bondy, A.L., Dutcher, C.S., Shepson, P.B. and Ault, A.P., 2016. Direct measurement of pH in individual particles via Raman microspectroscopy and variation in acidity with relative humidity. The Journal of Physical Chemistry A, 120(6), pp.911-917.

Rood, M.J., Shaw, M.A., Larson, T.V. and Covert, D.S., 1989. Ubiquitous nature of ambient metastable aerosol. Nature, 337(6207), pp.537-539.

Seinfeld, J. and Pandis, S., 2008. Atmospheric Chemistry and Physics. 1997. New York.

Shi, G., Xu, J., Peng, X., Xiao, Z., Chen, K., Tian, Y., Guan, X., Feng, Y., Yu, H., Nenes, A. and Russell, A.G., 2017. pH of aerosols in a polluted atmosphere: source contributions to highly acidic aerosol. Environmental science & technology, 51(8), pp.4289-4296.

Sinha, B. and Sinha, V., 2019. Source apportionment of volatile organic compounds in the northwest Indo-Gangetic Plain using a positive matrix factorization model. Atmospheric Chemistry and Physics, 19(24), pp.15467-15482.

Song, S., Gao, M., Xu, W., Shao, J., Shi, G., Wang, S., Wang, Y., Sun, Y. and McElroy, M.B., 2018. Fine-particle pH for Beijing winter haze as inferred from different thermodynamic equilibrium models. Atmospheric Chemistry and Physics, 18(10), pp.7423-7438.

Squizzato, S., Masiol, M., Brunelli, A., Pistollato, S., Tarabotti, E., Rampazzo, G. and Pavoni, B., 2013. Factors determining the formation of secondary inorganic aerosol: a case study in the Po Valley (Italy). Atmospheric chemistry and physics, 13(4), pp.1927-1939.

Toon, O.B., Hamill, P., Turco, R.P. and Pinto, J., 1986. Condensation of HNO3 and HCl in the winter polar stratospheres. Geophysical Research Letters, 13(12), pp.1284-1287.

Weber, R.J., Guo, H., Russell, A.G. and Nenes, A., 2016. High aerosol acidity despite declining atmospheric sulfate concentrations over the past 15 years. Nature Geoscience, 9(4), pp.282-285.

World Health Organization, 2016. Ambient air pollution: A global assessment of exposure and burden of disease.

Wu, Z., Wang, Y., Tan, T., Zhu, Y., Li, M., Shang, D., Wang, H., Lu, K., Guo, S., Zeng, L. and Zhang, Y., 2018. Aerosol liquid water driven by anthropogenic inorganic salts: Implying its key role in haze formation over the North China Plain. Environmental Science & Technology Letters, 5(3), pp.160-166.

Zhai, S., Jacob, D.J., Wang, X., Liu, Z., Wen, T., Shah, V., Li, K., Moch, J.M., Bates, K.H., Song, S. and Shen, L., 2021. Control of particulate nitrate air pollution in China. Nature Geoscience, 14(6), pp.389-395.

Zheng, G.J., Duan, F.K., Su, H., Ma, Y.L., Cheng, Y., Zheng, B., Zhang, Q., Huang, T., Kimoto, T., Chang, D.J.A.C. and Pöschl, U., 2015. Exploring the severe winter haze in Beijing: the impact of synoptic weather, regional transport and heterogeneous reactions. Atmospheric Chemistry and Physics, 15(6), pp.2969-2983.

References From the Supporting Information

Bian, Y.X., Zhao, C.S., Ma, N., Chen, J. and Xu, W.Y., 2014. A study of aerosol liquid water content based on hygroscopicity measurements at high relative humidity in the North China Plain. Atmospheric Chemistry and Physics, 14(12), pp.6417-6426.

Dusek, U., Frank, G.P., Curtius, J., Drewnick, F., Schneider, J., Kürten, A., Rose, D., Andreae, M.O., Borrmann, S. and Pöschl, U., 2010. Enhanced organic mass fraction and decreased hygroscopicity of cloud condensation nuclei (CCN) during new particle formation events. *Geophysical Research Letters*, *37*(3).

Engelhart, G.J., Hildebrandt, L., Kostenidou, E., Mihalopoulos, N., Donahue, N.M. and Pandis, S.N., 2011. Water content of aged aerosol. Atmospheric Chemistry and Physics, 11(3), pp.911-920.

Kim, Y.P., Seinfeld, J.H. and Saxena, P., 1993. Atmospheric gas-aerosol equilibrium I. Thermodynamic model. Aerosol Science and Technology, 19(2), pp.157-181.

Makkonen, U., Virkkula, A., Mäntykenttä, J., Hakola, H., Keronen, P., Vakkari, V. and Aalto, P.P., 2012. Semi-continuous gas and inorganic aerosol measurements at a Finnish urban site: comparisons with filters, nitrogen in aerosol and gas phases, and aerosol acidity. *Atmospheric Chemistry and Physics*, *12*(12), pp.5617-5631.

Malm, W.C. and Day, D.E., 2001. Estimates of aerosol species scattering characteristics as a function of relative humidity. Atmospheric Environment, 35(16), pp.2845-2860.

Murphy, J.G., Gregoire, P.K., Tevlin, A.G., Wentworth, G.R., Ellis, R.A., Markovic, M.Z. and VandenBoer, T.C., 2017. Observational constraints on particle acidity using measurements and modelling of particles and gases. Faraday discussions, 200, pp.379-395.

Petters, M.D. and Kreidenweis, S.M., 2007. A single parameter representation of hygroscopic growth and cloud condensation nucleus activity. *Atmospheric Chemistry and Physics*, *7*(8), pp.1961-1971.

Rumsey, I.C., Cowen, K.A., Walker, J.T., Kelly, T.J., Hanft, E.A., Mishoe, K., Rogers, C., Proost, R., Beachley, G.M., Lear, G. and Frelink, T., 2014. An assessment of the performance of the Monitor for AeRosols and GAses in ambient air (MARGA): a semi-continuous method for soluble compounds. Atmospheric Chemistry and Physics, 14(11), pp.5639-5658..

Rood, M.J., Shaw, M.A., Larson, T.V. and Covert, D.S., 1989. Ubiquitous nature of ambient metastable aerosol. Nature, 337(6207), pp.537-539.

Salcedo, D., Onasch, T.B., Dzepina, K., Canagaratna, M.R., Zhang, Q., Huffman, J.A., DeCarlo, P.F., Jayne, J.T., Mortimer, P., Worsnop, D.R. and Kolb, C.E., 2006. Characterization of ambient aerosols in Mexico City during the MCMA-2003 campaign with Aerosol Mass Spectrometry: results from the CENICA Supersite. *Atmospheric Chemistry and Physics*, *6*(4), pp.925-946.

Sjogren, S., Gysel, M., Weingartner, E., Baltensperger, U., Cubison, M.J., Coe, H., Zardini, A.A., Marcolli, C., Krieger, U.K. and Peter, T., 2007. Hygroscopic growth and water uptake kinetics of two-phase aerosol particles consisting of ammonium sulfate, adipic and humic acid mixtures. Journal of Aerosol Science, 38(2), pp.157-171.

Schaap, M., Otjes, R.P. and Weijers, E.P., 2011. Illustrating the benefit of using hourly monitoring data on secondary inorganic aerosol and its precursors for model evaluation. Atmospheric Chemistry and Physics, 11(21), pp.11041-11053.

Stanier, C.O., Khlystov, A.Y., Chan, W.R., Mandiro, M. and Pandis, S.N., 2004. A Method for the In Situ Measurement of Fine Aerosol Water Content of Ambient Aerosols: The Dry-Ambient Aerosol Size Spectrometer (DAASS) Special Issue of Aerosol Science and Technology on Findings from the Fine Particulate Matter Supersites Program. *Aerosol science and technology*, *38*(S1), pp.215-228.

Stokes, R.H. and Robinson, R.A., 1966. Interactions in aqueous nonelectrolyte solutions. I. Solute-solvent equilibria. The Journal of Physical Chemistry, 70(7), pp.2126-2131.

Su, H., Cheng, Y. and Pöschl, U., 2020. New Multiphase Chemical Processes Influencing Atmospheric Aerosols, Air Quality, and Climate in the Anthropocene. *Accounts of Chemical Research*, *53*(10), pp.2034-2043.

Sudheer, A.K. and Rengarajan, R., 2015. Time-resolved inorganic chemical composition of fine aerosol and associated precursor gases over an urban environment in western India: gas-aerosol equilibrium characteristics. Atmospheric Environment, 109, pp.217-227.

Tilgner, A., Schaefer, T., Alexander, B., Barth, M., Collett Jr, J.L., Fahey, K.M., Nenes, A., Pye, H.O., Herrmann, H. and McNeill, V.F., 2021. Acidity and the multiphase chemistry of atmospheric aqueous particles and clouds. Atmospheric Chemistry and Physics Discussions, pp.1-82.

Wang, Y. and Chen, Y., 2019. Significant climate impact of highly hygroscopic atmospheric aerosols in Delhi, India. Geophysical Research Letters, 46(10), pp.5535-5545.

Xu, L., Guo, H., Boyd, C.M., Klein, M., Bougiatioti, A., Cerully, K.M., Hite, J.R., Isaacman-VanWertz, G., Kreisberg, N.M., Knote, C. and Olson, K., 2015. Effects of anthropogenic emissions on aerosol formation from isoprene and monoterpenes in the southeastern United States. *Proceedings of the National Academy of Sciences*, *112*(1), pp.37-42.

Yao, X., Ling, T.Y., Fang, M. and Chan, C.K., 2007. Size dependence of in situ pH in submicron atmospheric particles in Hong Kong. Atmospheric Environment, 41(2), pp.382-393.

Ziemba, L.D., Fischer, E., Griffin, R.J. and Talbot, R.W., 2007. Aerosol acidity in rural New England: Temporal trends and source region analysis. Journal of Geophysical Research: Atmospheres, 112(D10).

Figure captions:

Figure 1: Comparison of ISORROPIA-II predicted and MARGA-2S measured NH_4^+, NO_3^-, and Cl^- of PM_1 (a, b, c) and $PM_{2.5}$ (d, e, f), gas-phase NH_3 (g) and (h) gas-to-particle partitioning ratio [(NH_4^+)]. The correlation (r) between the predicted and measured species concentrations are shown to check the validity of the model prediction. Data are color-coded by ambient air temperature (T).

Figure 2: The variability of gas-to-particle partitioning ratio of (a) (NO_3^-), (b) (Cl^-) with pH shown by the sigmoidal (S) curves. Three regimes are defined, where (NO_3^-) and (Cl^-) range between complete gas-phase ($= 0$; regime I) and complete particle-phase ($= 100\%$; regime III). A definite pH value called pH_{50} has been defined where total nitrate and chloride remained 50% in gas-phase and 50% in particle-phase (regime II). In figures c and d, we included ammonia (NH_4^+) phase-partitioning for PM_1 and $PM_{2.5}$ and defined the "sensitivity regimes" expressed in different colors. The particle phase fractions are sensitive to precursor concentrations HCl, HNO_3 and NH_3 and (NO_3^-) (blue curve), (Cl^-) (green curve), and (NH_4^+) (red curve) vary as a function of pH.

Figure 3: Chemical regimes of aerosols with "coordinates" being pH and aerosol liquid water content (ALWC) of PM_1 (a,b) and $PM_{2.5}$ (c,d). Aerosols are sensitive to HCl, HNO_3, and NH_3 concentrations and the black, blue, and red lines

define the "characteristic pH" where chemical regimes are separated by a predefined threshold value of = 10%. Above pH', pH", and pH'" the aerosols are sensitive to the variation in precursors like HCl, HNO_3, and NH_3, and below which aerosols are deemed insensitive to variations in precursors. The data points in b, d are colored by mass concentrations of PM_1 and $PM_{2.5}$ monitored during the WiFEX 2017-18 campaign period.

Figure 4: Schematic description of intrinsic physical, chemical, and thermodynamical mechanisms of fine aerosols during winter. The influences of aerosol acidity (pH) and aerosol liquid water content (ALWC) on the phase partitioning of total chloride (HCl + Cl^-), total nitrate (HNO_3 + NO_3^-), and total ammonium (NH_3 + NH_4^+) are shown during two conditions, clear sky and polluted atmosphere. Photochemistry dominates during the clean atmosphere, whereas heterogeneous, multiphase chemistry dominates during the polluted atmosphere. The particle-phase of chloride, nitrate, and gas-phase of ammonia dominates during winter over the Indo-Gangetic Plain (IGP).

Supporting Online Material

Abating HCl and HNO_3 is more effective than NH_3 for mitigating high aerosol loading over the Indo-Gangetic Plain

Prodip Acharja[1,2], Sachin D. Ghude[1*], Baerbel Sinha[3*], Mary Barth[4], Rachana Kulkarni[2], Vinayak Sinha[3], Rajesh Kumar[4], Kaushar Ali[1], Gaurav Govardhan[1], Ismail Gultepe[5,6,7], Madhavan Nair Rajeevan[8]

[1]Indian Institute of Tropical Meteorology, Ministry of Earth Sciences, India

[2]Savitribai Phule Pune University, Pune, India 411007

[3]Department of Earth and Environmental Sciences, Indian Institute of Science Education and Research Mohali, Punjab, India

[4]National Center for Atmospheric Research, Boulder, CO, 80307, USA

[5]ECCC, Meteorological Research Division, Toronto, Ontario, Canada

[6]Ontario Technical University, Engineering and Applied Science, Oshawa, Ontario, Canada

[7]Istinye University, Faculty of Engineering, Istanbul, Turkey

[8]Ministry of Earth Science, Lodhi Road, New Delhi, India

This file includes

Supplementary text

Table S1

Figure S1

Supporting Text

1. Data and measurements

1.1 Measurement site

The gas and particle-phase species measurements were conducted at the Indira Gandhi International Airport (IGIA), Delhi (28.56° N, 77.09°E, 237 m asl) under the Winter Fog Experiment (WiFEX) field campaign (Ghude et al., 2017). The measurement site fairly represents the general characteristics of highly polluted and densely populated urban locations in the IGP (Sinha et al., 2019; Ali et al., 2019). The measurements were conducted from 19 December 2017 to 10 February 2018 and a detailed description of the observation site and the prominent weather features associated with the winter period in Delhi has been well described in our earlier publications Ali et al., 2019; Acharja et al., 2021.

1.2 Instrumentation

1.2.1 Measurements of trace gases and inorganic constituents of PM_1, $PM_{2.5}$

In this study, the measurement of trace gases (HCl, HONO, HNO_3, SO_2, and NH_3) and the inorganic constituents (Cl^-, NO_3^-, SO_4^{2-}, Na^+, NH_4^+, K^+, Ca^{2+}, and Mg^{2+}) of fine particulates (PM_1 and $PM_{2.5}$) were simultaneously conducted at hourly resolution using Monitor for Aerosol and Gases in ambient Air (MARGA-2S, Make: Metrohm Applikon B.V, Netherlands) instrument (Rumsey et al., 2014).

The instrument is an assembly of equipment consisting of sampling unit, denuder for separating trace gases from the particles, aerosol collector, and analytical unit (Makkonen et al., 2012). MARGA-2S can provide a physicochemical characterization of particle matter along with trace gases on hourly time resolution (Schaap et al., 2011). In the measurement system, ambient air is first drawn through the PM_1, $PM_{2.5}$ inlets that pass through horizontal wet rotating denuder (WRD), and gases get diffused into an aqueous film. The aerosol gets collected in the steam jet aerosol collector (SJAC), where water-soluble aerosols grow in a supersaturated environment (Stieger et al., 2018). The water-soluble inorganic ions are quantified with two ion chromatography systems (anion + cation) using the principle presented by Oms et al., 1996. The MARGA-2S instrument was installed on the first floor of the building, whereas PM_1 and $PM_{2.5}$ impactors were installed on the terrace of the building nearly 8m above the ground and 2m above the roof surface. The instrument was continuously calibrated during its operation to ensure the quality of observation. A detailed description of

the MARGA-2S instrument, its operating principle, calibration method, and study location is discussed in our previous publication (Acharja et al., 2021). Meteorological parameters like temperature, relative humidity, wind speed, and wind direction were monitored with co-located automatic weather station (AWS).

2. Methodology

2.1 Thermodynamic equilibrium model ISORROPIA-II

The thermodynamic state of aerosols depends on ionic strength, dissociation of electrolyte, temperature of the solution, pH of aerosol, water activity, surface tension, density, and hygroscopicity (Kim et al., 1993; Tilgner et al., 2021). In the present study, ISORROPIA-II (Cl^- - NO_3^- - SO_4^{2-} - NH_4^+ - Na^+ - K^+ - Mg^{2+} - Ca^{2+} - H_2O system) model was used (Fountoukis and Nenes, 2007; Weber et al., 2016; Liu et al., 2017). In the model, the equilibrium is characterized by simultaneously considering a set of nonlinear algebraic equations coupled with appropriate electro-neutrality and mass conservation equations using the Newton-Raphson and bisectional methods (Ansari and Pandis., 1999). It is also assumed that the system is closed with respect to the total constituents, and the Gibbs free energy is at the global minimum. At this state, the variation in entropy concerning neighboring states is zero, and the system may remain at this energy level for arbitrarily long times.

The observational dataset of concentration of total ammonium ($TNH_4=NH_3 + NH_4^+$), total nitrate ($TNO_3=HNO_3 + NO_3^-$), and total chloride ($TCl=HCl + Cl^-$) along with Na^+, K^+, Ca^{2+}, and Mg^{2+} were used as inputs to run the model. The model can run in the "backward" mode based on the particle-phase data and in the "forward" mode based on the total (particle + gas) phase concentration data (Xu et al., 2015; Yao et al., 2007; Guo et al., 2017; Song et al., 2007). Studies have shown the "forward" mode to be more accurate and less sensitive to the measurement uncertainties compared to the "backward" mode (Hennigan et al., 2015; Bian et al., 2014). In the "forward" mode, the aerosols are assumed to exist in a metastable or aqueous state. These aqueous particles being larger than dry crystalline solids, generally scatter more light, degrade visibility, and influence mass transfer kinetics of trace gases (Rood et al., 1989).

The particle acidity (pH) is estimated using the following equation:

$$pH = -log_{10}\frac{1000 \times [H_{air}^+]}{ALWC} \quad (1)$$

where $[H_{air}^+]$ concentration and aerosol liquid water content (ALWC) are the ISORROPIA-II model outputs (Liu et al., 2014; Xue et al., 2011). In the model, the ALWC was estimated by

considering the Raoult effect, curvature effect, and water uptake property (Bian et al., 2014; Hennigan et al., 2008). The water uptake of aerosols is calculated with the Zdanovskii–Stokes–Robinson (ZSR) hypothesis (Stokes and Robinson, 1966)

$$A = \sum_i \frac{M_i}{m_{oi}\ (a_w)} \qquad (2)$$

where M_i is the mole concentration of the electrolyte i (mol m^{-3}), $m_{oi}(a_w)$ is the corresponding molality of the binary solution of the electrolyte i under the same a_w (Seinfeld and Pandis, 2006). At the phase equilibrium a_w is equal to the ambient RH:

$$a_w = RH \qquad (3)$$

This approach ignores the contribution of organic species (e.g., oxalate, formate, acetate) to ALWC, but studies have shown that organics do not significantly affect the aerosol liquid water content (Ziemba et al., 2007; Malm and Day, 2001).

In this study, the data of RH in the 30–95% range were considered for the model simulation and data of RH > 95% were excluded since the exponential growth in ALWC with RH introduces large pH uncertainties (Guo et al., 2015). During the study period, the ambient humidity was high (≥50%), much higher than the efflorescence RH (10-30 %), so the "forward" mode consideration and the assumption that aerosols were in a completely deliquesced phase and remained at the "metastable" side of the hysteresis is reasonable. The model-derived pH of $PM_{2.5}$ was compared to make a comprehensive analysis of the model simulation.

2.2 Gas-particle partitioning ratio

The gas-to-particle partitioning and formation of secondary aerosols are significantly impacted by pH, ALWC, and T. High ALWC results in uptake of a gaseous species onto liquid and phase partitioning depending on the multiphase and heterogeneous reaction rates and the measurement or module of the model used (Nemitz et al., 2004; Hanson et al., 1994; Murphy et al., 2017). The partitioning ratio of ammonium [$\varepsilon(NH_4^+)$], nitrate [$\varepsilon(NO_3^-)$], and chloride [$\varepsilon(Cl^-)$] can be estimated using the following equations:

$$\varepsilon(NH_4^+) = \frac{[NH_4^+]}{[NH_3] + [NH_4^+]} \qquad (4)$$

$$\varepsilon(NO_3^-) = \frac{[NO_3^-]}{[HNO_3] + [NO_3^-]} \qquad (5)$$

$$\varepsilon(Cl^-) = \frac{[Cl^-]}{[HCl] + [Cl^-]} \quad (6)$$

where $[NH_4^+]$, $[NO_3^-]$, $[Cl^-]$, $[NH_3]$, $[HNO_3]$, [HCl] are the molar concentrations (μmol m^{-3}) of particulate and gaseous species respectively. The agreement between the predicted and measured partitioning ratios has been evaluated by estimating the mean bias (MB) and normalized mean bias (NMB) using the following equations:

$$MB = \frac{1}{N} \times \sum_{i=1}^{N} (M_i - O_i) \quad (7)$$

$$NMB = \frac{\sum_{i=1}^{N} (M_i - O_i)}{\sum_{i=1}^{N} O_i} \times 100\% \quad (8)$$

where, M_i and O_i are the model predicted and observed data, respectively, and N is the number of data points (Sudheer et al., 2015). These metrics are commonly used to evaluate the model predictions, and negative values for MB and NMB imply lower prediction, whereas positive values show the over-prediction.

2.3 Volume growth factor (VGF)

Factors like pH, ALWC, RH, aerosol composition, aerosol size, and aging of aerosol play an important role in visibility degradation by impacting the growth of hygroscopic aerosols (Stainer et al., 2003; Salcedo et al., 2006). The volume growth factor (VGF) is defined as the ratio of the volume of the wet particle to the corresponding volume of the dry particle (Zheng et al., 2015; Sun et al., 2013). Li et al., (2019) have discussed the size-independent VGF estimated using the following equation:

$$VGF = \frac{\frac{\sum m_{i.\ MARGA}}{\rho_i} + (\frac{ALWC_{inorg} + ALWC_{org})}{\rho_{water}}}{\frac{\sum m_{i.\ MARGA}}{\rho_i}} \quad (9)$$

where m_{iMARGA} is the mass concentration of species 'i' measured by MARGA-2S. In this calculation, we have also neglected the impact of organic fraction as studies have shown their growth is much less than water-soluble inorganic ions (Dusek et al., 2010; Petters and Kreidenweis, 2007; Guo et al., 2015). The major inorganic species are considered in the calculation, and the densities were assumed to be 1.52, 1.75, 1.75, 1.75, and 1.0 g cm^{-3} for chloride, nitrate, sulfate, ammonium, and water respectively (Salcedo et al., 2006).

3. Results and Discussions

3.1 Temporal evolution of pH and ALWC of PM_1 and $PM_{2.5}$

We explored the diurnal variation of pH and ALWC of PM_1 and $PM_{2.5}$ in Figure S1. ALWC increases from just after sunset to early morning, then decreases sharply due to daytime heating, increasing temperature, and decreasing RH. It reaches a maximum during morning traffic hours (08:00-10:00 hrs) due to high loadings of PM_1, $PM_{2.5}$ and high humidity in the shallow boundary layer. It was lowest in the afternoon, due to the combined effect of temperature and increased boundary layer height, which dilutes the particle concentration at the ground level, consistent with the variations in other polluted regions experiencing fog (Guo et al., 2018). The pH variation generally followed the variation of liquid water content and it showed a double peak, one in the morning (10:00 hrs), and another in the evening (20:00 hrs), as shown in Figure S1. It was minimum in the afternoon, similar to ALWC, and studies have shown the diurnal variation of ALWC to be the primary driving factor in the diurnal variation of pH.

3.2 Influence of RH and ALWC on volume growth factor (VGF)

In addition to controlling the pH of aerosols, ALWC also impacts the loading of aerosols where higher aerosol concentration increases ALWC content, further enhancing the multiphase formation of aerosol, especially when RH exceeded ≥ 80% resulting in the growth of aerosol during pollution events like fog (Su et al., 2020; Engelhart et al., 2011; Liu et al., 2011; Zhai et al., 2021). Limited research has been performed on this topic over IGP though the highest RH value was beyond 90% during the winter period.

Figures 3c, 3d give a clear view of VGF variability with RH. The figure shows that VGF of both PM_1 and $PM_{2.5}$ increased sharply when ambient RH was ≥ 70%, which is due to the water uptake by hygroscopic constituents. Below 70% RH, the mean PM_1 and $PM_{2.5}$ VGF is 2.02 ± 0.77, 2.08 ± 0.97, whereas at RH ≥ 70% the mean PM_1 and $PM_{2.5}$ VGF is 7.87 ± 4.58, 7.38 ± 4.46 respectively. This indicates the increment of VGF by 70% at higher RH, which can be attributed to the increased phase partitioning and formation of more SIA under fog (Sjogren et al., 2007; Wang et al., 2019).

During the whole measurement period, the average VGF of PM_1 and $PM_{2.5}$ was 4.83 ± 4.21, 5.05 ± 4.44 showing nearly 5 times increase in the volume of foggy particles compared to the particle volume at non-foggy conditions, which is consistent with previous studies (Bian et al., 2014). The increase in VGF of $PM_{2.5}$ aerosols was more compared to PM_1 as it has a larger volume fraction. This increased volume of particles at high RH would augment the particle mass loading, resulting in scattering more sunlight and lowering the surface temperature, and increasing fog sustenance. This results in a positive feedback

mechanism between RH and VGF that would reach equilibrium at some ALWC and pH (Wang et al., 2014; Guo et al. 2017).

Table S1. The measured total (gas + aerosol) concentration of chloride (TCl), nitrate (TNO_3), and ammonia (TNH_4) and estimated pH, ALWC, gas-to-particle partitioning ratio (ε) of ε (Cl^-), ε (NO_3^-), and ε (NH_4^+) of PM_1 and $PM_{2.5}$ during the WiFEX campaign period.

Variables	PM_1	$PM_{2.5}$
TNO_3 (μg m^{-3})	19.74 ± 9.81	31.67 ± 14.57
TCl (μg m^{-3})	22.28 ± 20.57	39.71 ± 35.41
TNH_4 (μg m^{-3})	43.41 ± 19.81	58.04 ± 24.06
Gas-to-particle partitioning ratio (ε)		
ε (Cl^-)	93 ± 09 %	96 ± 07 %
ε(NO_3-)	83 ± 11 %	89 ± 08 %
ε (NH_4^+)	42 ± 17 %	55 ± 15 %
Predicted from ISORROPIA-II		
pH	4.49 ± 0.53	4.58 ± 0.48
ALWC (μg m^{-3})	169 ± 205	324 ± 396

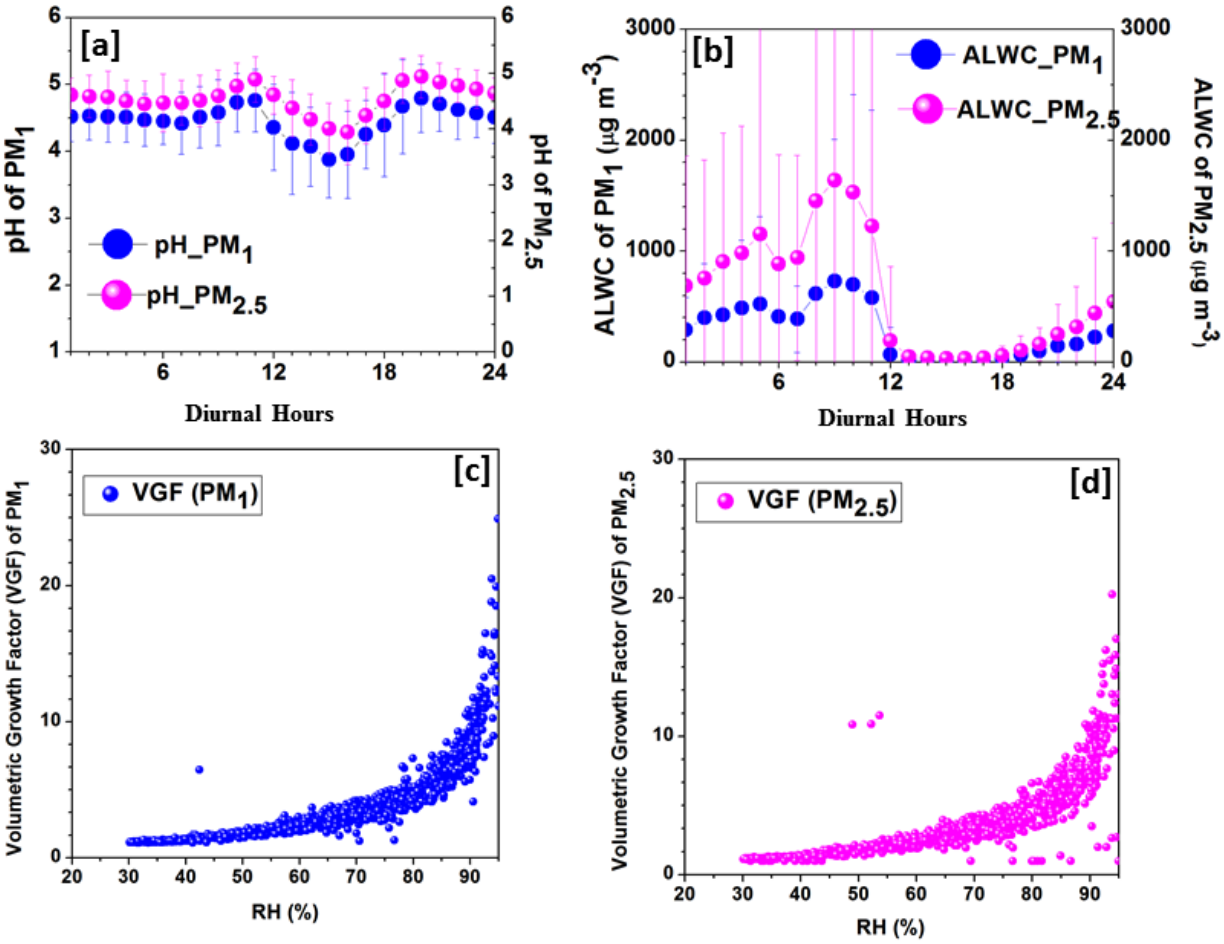

Figure S1: Diurnal variation of (a) pH and (b) ALWC of PM_1 and $PM_{2.5}$ predicted from the ISORROPIA-II model simulation. Variation of volume growth factor (VGF) of (c) PM_1 and (d) $PM_{2.5}$ as a function of RH during the WiFEX campaign period.

References

Acharja, P., Ali, K., Trivedi, D.K., Safai, P.D., Ghude, S., Prabhakaran, T. and Rajeevan, M., 2020. Characterization of atmospheric trace gases and water soluble inorganic chemical ions of PM1 and PM2. 5 at Indira Gandhi International Airport, New Delhi during 2017–18 winter. Science of the Total Environment, 729, p.138800.

Acharja, P., Ali, K., Ghude, S.D., Sinha, V., Sinha, B., Kulkarni, R., Gultepe, I. and Rajeevan, M.N., 2021. Enhanced secondary aerosol formation driven by excess ammonia during fog episodes in Delhi, India. Chemosphere, p.133155.

Ali, K., Acharja, P., Trivedi, D.K., Kulkarni, R., Pithani, P., Safai, P.D., Chate, D.M., Ghude, S., Jenamani, R.K. and Rajeevan, M., 2019. Characterization and source identification of PM2. 5 and its chemical and carbonaceous constituents during Winter Fog Experiment 2015–16 at Indira Gandhi International Airport, Delhi. Science of The Total Environment, 662, pp.687-696.

Ansari, A.S. and Pandis, S.N., 2000. The effect of metastable equilibrium states on the partitioning of nitrate between the gas and aerosol phases. Atmospheric Environment, 34(1), pp.157-168.

Bian, Y.X., Zhao, C.S., Ma, N., Chen, J. and Xu, W.Y., 2014. A study of aerosol liquid water content based on hygroscopicity measurements at high relative humidity in the North China Plain. Atmospheric Chemistry and Physics, 14(12), pp.6417-6426.

Dusek, U., Frank, G.P., Curtius, J., Drewnick, F., Schneider, J., Kürten, A., Rose, D., Andreae, M.O., Borrmann, S. and Pöschl, U., 2010. Enhanced organic mass fraction and decreased hygroscopicity of cloud condensation nuclei (CCN) during new particle formation events. *Geophysical Research Letters*, *37*(3).

Engelhart, G.J., Hildebrandt, L., Kostenidou, E., Mihalopoulos, N., Donahue, N.M. and Pandis, S.N., 2011. Water content of aged aerosol. Atmospheric Chemistry and Physics, 11(3), pp.911-920.

Guo, H., Otjes, R., Schlag, P., Kiendler-Scharr, A., Nenes, A. and Weber, R.J., 2018. Effectiveness of ammonia reduction on control of fine particle nitrate. Atmospheric Chemistry and Physics, 18(16), pp.12241-12256.

Hanson, D.R., Ravishankara, A.R. and Solomon, S., 1994. Heterogeneous reactions in sulfuric acid aerosols: A framework for model calculations. *Journal of Geophysical Research: Atmospheres*, *99*(D2), pp.3615-3629.

Hennigan, C.J., Izumi, J., Sullivan, A.P., Weber, R.J. and Nenes, A., 2015. A critical evaluation of proxy methods used to estimate the acidity of atmospheric particles. Atmospheric Chemistry and Physics, 15(5), pp.2775-2790.

Kim, Y.P., Seinfeld, J.H. and Saxena, P., 1993. Atmospheric gas-aerosol equilibrium I. Thermodynamic model. Aerosol Science and Technology, 19(2), pp.157-181.

Liu, M., Song, Y., Zhou, T., Xu, Z., Yan, C., Zheng, M., Wu, Z., Hu, M., Wu, Y. and Zhu, T., 2017. Fine particle pH during severe haze episodes in northern China. Geophysical Research Letters, 44(10), pp.5213-5221.

Makkonen, U., Virkkula, A., Mäntykenttä, J., Hakola, H., Keronen, P., Vakkari, V. and Aalto, P.P., 2012. Semi-continuous gas and inorganic aerosol measurements at a Finnish urban site: comparisons with filters, nitrogen in aerosol and gas phases, and aerosol acidity. *Atmospheric Chemistry and Physics*, *12*(12), pp.5617-5631.

Malm, W.C. and Day, D.E., 2001. Estimates of aerosol species scattering characteristics as a function of relative humidity. Atmospheric Environment, 35(16), pp.2845-2860.

Murphy, J.G., Gregoire, P.K., Tevlin, A.G., Wentworth, G.R., Ellis, R.A., Markovic, M.Z. and VandenBoer, T.C., 2017. Observational constraints on particle acidity using measurements and modelling of particles and gases. Faraday discussions, 200, pp.379-395.

Petters, M.D. and Kreidenweis, S.M., 2007. A single parameter representation of hygroscopic growth and cloud condensation nucleus activity. *Atmospheric Chemistry and Physics*, *7*(8), pp.1961-1971.

Rumsey, I.C., Cowen, K.A., Walker, J.T., Kelly, T.J., Hanft, E.A., Mishoe, K., Rogers, C., Proost, R., Beachley, G.M., Lear, G. and Frelink, T., 2014. An assessment of the performance of the Monitor for AeRosols and GAses in ambient air (MARGA): a semi-continuous method for soluble compounds. Atmospheric Chemistry and Physics, 14(11), pp.5639-5658..

Rood, M.J., Shaw, M.A., Larson, T.V. and Covert, D.S., 1989. Ubiquitous nature of ambient metastable aerosol. Nature, 337(6207), pp.537-539.

Salcedo, D., Onasch, T.B., Dzepina, K., Canagaratna, M.R., Zhang, Q., Huffman, J.A., DeCarlo, P.F., Jayne, J.T., Mortimer, P., Worsnop, D.R. and Kolb, C.E., 2006. Characterization of ambient aerosols in Mexico City during the MCMA-2003 campaign with Aerosol Mass Spectrometry: results from the CENICA Supersite. *Atmospheric Chemistry and Physics*, *6*(4), pp.925-946.

Sjogren, S., Gysel, M., Weingartner, E., Baltensperger, U., Cubison, M.J., Coe, H., Zardini, A.A., Marcolli, C., Krieger, U.K. and Peter, T., 2007. Hygroscopic growth and water uptake kinetics of two-phase aerosol particles consisting of ammonium sulfate, adipic and humic acid mixtures. Journal of Aerosol Science, 38(2), pp.157-171.

Sinha, B. and Sinha, V., 2019. Source apportionment of volatile organic compounds in the northwest Indo-Gangetic Plain using a positive matrix factorization model. Atmospheric Chemistry and Physics, 19(24), pp.15467-15482.

Schaap, M., Otjes, R.P. and Weijers, E.P., 2011. Illustrating the benefit of using hourly monitoring data on secondary inorganic aerosol and its precursors for model evaluation. Atmospheric Chemistry and Physics, 11(21), pp.11041-11053.

Song, S., Gao, M., Xu, W., Shao, J., Shi, G., Wang, S., Wang, Y., Sun, Y. and McElroy, M.B., 2018. Fine-particle pH for Beijing winter haze as inferred from different

thermodynamic equilibrium models. *Atmospheric Chemistry and Physics*, *18*(10), pp.7423-7438.

Stanier, C.O., Khlystov, A.Y., Chan, W.R., Mandiro, M. and Pandis, S.N., 2004. A Method for the In Situ Measurement of Fine Aerosol Water Content of Ambient Aerosols: The Dry-Ambient Aerosol Size Spectrometer (DAASS) Special Issue of Aerosol Science and Technology on Findings from the Fine Particulate Matter Supersites Program. *Aerosol science and technology*, *38*(S1), pp.215-228.

Stokes, R.H. and Robinson, R.A., 1966. Interactions in aqueous nonelectrolyte solutions. I. Solute-solvent equilibria. The Journal of Physical Chemistry, 70(7), pp.2126-2131.

Su, H., Cheng, Y. and Pöschl, U., 2020. New Multiphase Chemical Processes Influencing Atmospheric Aerosols, Air Quality, and Climate in the Anthropocene. *Accounts of Chemical Research*, *53*(10), pp.2034-2043.

Sudheer, A.K. and Rengarajan, R., 2015. Time-resolved inorganic chemical composition of fine aerosol and associated precursor gases over an urban environment in western India: gas-aerosol equilibrium characteristics. Atmospheric Environment, 109, pp.217-227.

Tilgner, A., Schaefer, T., Alexander, B., Barth, M., Collett Jr, J.L., Fahey, K.M., Nenes, A., Pye, H.O., Herrmann, H. and McNeill, V.F., 2021. Acidity and the multiphase chemistry of atmospheric aqueous particles and clouds. Atmospheric Chemistry and Physics Discussions, pp.1-82.

Wang, Y. and Chen, Y., 2019. Significant climate impact of highly hygroscopic atmospheric aerosols in Delhi, India. Geophysical Research Letters, 46(10), pp.5535-5545.

Weber, R.J., Guo, H., Russell, A.G. and Nenes, A., 2016. High aerosol acidity despite declining atmospheric sulfate concentrations over the past 15 years. *Nature Geoscience*, *9*(4), pp.282-285.

Xu, L., Guo, H., Boyd, C.M., Klein, M., Bougiatioti, A., Cerully, K.M., Hite, J.R., Isaacman-VanWertz, G., Kreisberg, N.M., Knote, C. and Olson, K., 2015. Effects of anthropogenic emissions on aerosol formation from isoprene and monoterpenes in the southeastern United States. *Proceedings of the National Academy of Sciences*, *112*(1), pp.37-42.

Yao, X., Ling, T.Y., Fang, M. and Chan, C.K., 2007. Size dependence of in situ pH in submicron atmospheric particles in Hong Kong. Atmospheric Environment, 41(2), pp.382-393.

Ziemba, L.D., Fischer, E., Griffin, R.J. and Talbot, R.W., 2007. Aerosol acidity in rural New England: Temporal trends and source region analysis. Journal of Geophysical Research: Atmospheres, 112(D10).